Published in final edited form as:
J Ultrasound Med. 2008 June ; 27(6): 895–905.

Three-Dimensional Sonography With Needle Tracking:

Role in Diagnosis and Treatment of Prostate Cancer

Feimo Shen, PhD, **Katsuto Shinohara, MD**, **Dinesh Kumar, MS**, **Animesh Khemka, MS**, **Anne R. Simoneau, MD**, **Priya N. Werahera, PhD**, **Lu Li, MS**, **Yujun Guo, PhD**, **Ramkrishnan Narayanan, PhD**, **Liyang Wei, PhD**, **Al Barqawi, MD**, **E. David Crawford, MD**, **Christos Davatzikos, PhD**, and **Jasjit S. Suri, PhD**
Eigen LLC, Grass Valley, California USA (F.S., D.K., A.K., L.L., Y.G., R.N., L.W., J.S.S.); University of California, San Francisco, California USA (K.S.); University of California, Irvine, California USA (A.R.S.); University of Colorado, Denver, Colorado USA (P.N.W., A.B., E.D.C.); and University of Pennsylvania, Philadelphia, Pennsylvania USA (C.D.).

Abstract

Objective—Image-guided prostate biopsy has become routine in medical diagnosis. Although it improves biopsy outcome, it mostly operates in 2 dimensions, therefore lacking presentation of information in the complete 3-dimensional (3D) space. Because prostatic carcinomas are nonuniformly distributed within the prostate gland, it is crucial to accurately guide the needles toward clinically important locations within the 3D volume for both diagnosis and treatment.

Methods—We reviewed the uses of 3D image-guided needle procedures in prostate cancer diagnosis and cancer therapy as well as their advantages, work flow, and future directions.

Results—Guided procedures for the prostate rely on accurate 3D target identification and needle navigation. This 3D approach has potential for better disease diagnosis and therapy. Additionally, when fusing together different imaging modalities and cancer probability maps obtained from a population of interest, physicians can potentially place biopsy needles and other interventional devices more accurately and efficiently by better targeting regions that are likely to host cancerous tissue.

Conclusions—With the information from anatomic, metabolic, functional, biochemical, and biomechanical statuses of different regions of the entire gland, prostate cancers will be better diagnosed and treated with improved work flow.

Keywords

diagnosis; multimodality image fusion; prostate cancer; 3-dimensional sonography

Prostate cancer is the most common type of cancer and the second leading cause of cancer death in men in the United States.[1] It is a very prevalent disease, as 1 per 6 men in the United States will have prostate cancer. Like other cancers, prostate cancer is curable when diagnosed early.[2] New cancer statistics have revealed a continuous decline in prostate cancer deaths in recent years, suggesting that early detection and treatment have had a major impact on this disease.[3,4] Accurate early diagnosis is crucial in clinical management of the disease and consequently patients' quality of life and life expectancy. In managing cases of possible prostate cancer, it is challenging to detect and stage clinically relevant cancer and apply

Address correspondence and reprint requests to Jasjit S. Suri, PhD, Eigen LLC, 13366 Grass Valley Ave, Grass Valley, CA 95945 USA. jas.suri@eigen.com.

optimal therapy. To achieve this objective, advanced imaging methods are necessary to determine the accurate grade and stage of the disease.[5,6] Advancements in ultrasound and other technologies and the potential benefits of information in full spatiotemporal dimensions motivated this review.

Screening for prostate cancer is performed by digital rectal examination and measurement of the serum prostate-specific antigen (PSA) level. However, abnormal digital rectal examination findings and elevated serum PSA levels (≥4 ng/mL) are not always indicative of prostate cancer. The reference standard for diagnosis of prostate cancer is pathologic confirmation of the disease from tissue biopsy.[7] To minimize invasiveness, a thin-needle biopsy is usually performed through the rectal wall while guided by transrectal sonography. The extracted tissue core is then processed for histologic analysis. The reading of the stained histopathology slides determines the presence of cancer, and a Gleason score is assigned to rate the aggressiveness of the cancer.[5]However, locations for needle insertion are determined by physician experience and are guided by simple 2-dimensional (2D) images produced by a handheld device. The 2D image informs the physician of the anatomy of the prostate so that the location and depth of the biopsy needle can be estimated in the gland. Consequently, random prostate biopsies are subjected to serious sampling errors. This biopsy process largely remains manual, and the lack of a positional tracker makes it inaccurate.

This inaccuracy causes patients physical and emotional burdens because current prostate needle biopsies have low specificity,[8,9] commonly leading to additional biopsies. To improve the detection rate, many physicians increase the number of biopsy cores to as many as 45.[10] In these situations, patients face increasing anxiety, discomfort, risk of rectal bleeding, risk of infection, and expenses. To alleviate this problem, better imaging techniques are needed to obtain and present the entire spatial information of the prostate in 3 dimensions.

New technologies that involve 3-dimensional (3D) image acquisition and computation are being introduced and gradually accepted in surgery. Application of these new imaging technologies enables physicians to have a better knowledge of the 3D spatial location of the gland and the locations of tumor sites. Three-dimensional systems let the operator target areas that are most likely to have cancer and to rebiopsy or reimage specific areas, something that is difficult to do with 2D imaging. Therefore, determination of the accurate grade and stage of disease can be improved appreciably compared with traditional 2D guidance.

The aim of this review was to survey the applications of 3D image-guided interventional procedures for prostate cancer diagnosis and treatment. Recent advances in locating optimal regions for detecting prostatic carcinoma include a cancer probability atlas,[11] magnetic resonance (MR) spectroscopy,[12] elastography,[13,14] and fusion of different imaging modalities. Advanced spatial tracking of images and biopsy needles ensures precise sampling and targeted therapy of cancer regions within the prostate gland. These advances result in substantially improved procedures to benefit patients with prostate cancer.

Information on 2D and 3D Imaging

Thus far, biopsies have been performed without information regarding the precise locations of the cores. Currently, physicians rely on conventional 2D sonographic images, which are generated by a handheld transducer probe. For example, a side-firing transrectal ultrasound (TRUS) probe can show either a sagittal or coronal view of the prostate but not both at the same time. Hence, the physician can only view a thin slice of the organ at a time (Figure 1A, prostate phantom), albeit in real time. The user must mentally integrate the sequences of the

2D images to form an impression of the 3D anatomy of the gland based on anatomic landmarks from the sonographic images. Furthermore, because the device is handheld without tracking, the exact location within the organ is not known, and finding the same location for reexamination is very difficult. Consequently, targeting diagnosed cancer for focal therapy as well as monitoring for recurrence is difficult.

To overcome this difficulty, 3D prostate image-guided procedures were investigated initially by Elliot et al[15] and Tong et al,[16] who tracked the positions of conventional ultrasound transducer probes to produce 3D images by reconstructing the 2D images from the probes. Subsequent studies have been published for improvement and validation of this procedure.[17–21] The TargetScan system (Envisioneering Medical Technologies, St Louis, MO) uses computer-directed needle biopsies based on anatomic landmarks within the prostate and computerized 3D reconstruction of the gland to identify small foci of cancer in a highly reproducible manner.[22,23] The device then allows the physician to insert a proprietary biopsy needle in the targeted area and monitor the accuracy of the needle position and the specific location of the tissue sample.

The Artemis system (Eigen LLC, Grass Valley, CA) provides real-time locations of the ultrasound probe so that the patient's prostate and the biopsy needle are well referenced in situ (Figure 2A). Unlike a side-firing probe, the end-firing probe that is held by an arm with 4° of freedom in this system can be rotated about a fulcrum (anus) every 3° with a range of 160° so that the entire prostate is fully traversed (Figure 2B). As the probe is rotated about its longitudinal axis, a full 3D image of the prostate is acquired by sequentially capturing axial images. After the acquisition, 3D image segmentation is performed so that the entire surface location is completely known.

Benefits of having the third dimension include shape and target traceability over time, 3D target planning and navigation guidance, accurate volume calculation, motion compensation, and improved work flow. With information readily available in the third dimension, physicians can more easily view the gland from different angles and more confidently track procedures using this interventional device. Figure 1 compares the traditional 2D and the new 3D image-guided biopsy procedures. Figure 1A shows coronal and sagittal views of a prostate phantom via a manual ultrasound machine. Figure 1, B and C, shows the 2 accurately segmented 3D models and planned biopsy locations for a current session based on input from a previous session. With this system, the prostate shape and biopsy core locations are traceable over time. Knowledge of the spatial 3D location and depth of cores and the ability to track over time provide important information for precise needle placement.

A tissue core obtained from an 18-gauge biopsy needle on average is 12 mm long with a 0.8-mm diameter.[11] The total core volume in a biopsy session is very small compared with the gland volume (<1%); therefore, the chance of intersecting the diseased portion of the organ is low for random or blind sampling of the prostate. Although there are known "hot spots" (locations with statistically high probability for prostate cancer), targeting such sites without 3D information, such as the prostate capsule surface and volume, is ineffective. Because of the low signal-to-noise ratio on sonograms and without a priori information about the cancer, blind sampling results in low specificity and sensitivity. Therefore, an accurate 3D display could play a dominant role in guiding the physician to obtain desired tissue samples from locations with a high probability of cancer.

An additional advantage of automated 3D computation is improved prostate volume calculations. Methods for prostate volume estimation include manual, semiautomatic, and automatic techniques. The traditional method is a calculation via measurements of the

length, width, and height of prostate image slices from 2D images, which have relatively high error rates.[24,25] Segmenting the prostate boundary leads to a defined space, so volume calculation is more accurate. Recent advances by Wang et al[20] used a semiautomatic discrete dynamic contour method for segmenting 2D slices from a 3D volume. The most recent methods were fully automatic using least squares and a level set.[26,27]When compared, the errors of the volume calculations were 1.0%, 0.8%, and 4.1% for the least squares, level set, and discrete dynamic contour algorithms, respectively.[28] Therefore, 3D image segmentation yields much better prostate volume estimation than traditional methods. With more accurate prostate volume information obtained, important parameters can be calculated to track disease progress. These parameters include the PSA density (PSA level divided by prostate volume) and its rate of change. The volume can also be used in nomograms to optimize the number of biopsies. The accuracy of these metrics is highly dependent on volume measurement and, in turn, image segmentation.

Despite the challenges of image acquisition and processing, the work flow of the needle core biopsy procedure can be standardized and improved. Three-dimensional imaging techniques are great tools for increasing the cancer detection rate by accurately informing the physician where to sample within the gland. Therefore, the physician no longer needs to “guess” where to place the needles. The work flow of the diagnosis and therapy procedures will be improved by increased efficiency when 3D images are systematically processed and analyzed with a tracking assembly such as that shown in Figure 2A. Subjective mental formatting to deduce information in the third dimension from 2D slices is replaced by simple navigation in the computer-generated 3D space.

Compared with the 2D methods, the new 3D method provides a new level of information that will systematically guide the physician to more accurately and safely sample the regions of greatest interest.

Cancer Probability Atlas– and 3D Atlas–Guided Biopsies

Because the probability of intersecting cancerous tissue with a few needles by chance is low, physicians attempt to improve the detection rate by strategizing needle placements and increasing the number of biopsy cores. A study by Paul et al[29] reported an increase of the prostate cancer detection rate from 32% for 6 cores to 40% for 10 cores, which added 2 median cores on both sides to their modified sextant biopsy. However, a study by Naughton et al[30] reported that only increasing the number of cores from 6 to 12 did not lead to any improvement. Yet, in another study by Chen et al,[31] an 11-core biopsy improved the detection rate to 85% and 70% for prostates of less than and greater than 50 g, respectively. In that study, instead of randomly increasing the cores, the multisite biopsy included 1 sextant, 1 posterior midline, 2 transition, and 2 anterior horn cores. Comparing these studies, it is strongly suggested that the location is a crucial factor in substantially improving detection rates. Knowing that the spatial distribution of cancer within the prostate is inhomogeneous,[31–33] spatially selective handling can improve detection rates considerably over traditional methods. Opell et al[34] developed a spatial distribution map of cancers in the prostate: They concluded that the cancers were more commonly found in the posterior half and the apical and mid regions of the prostate and suggested use of the map to develop more sophisticated biopsy protocols. A more accurate distribution of the spatial probability can be determined by examining a series of whole-mounted radical prostatectomy specimens for noting cancer locations in the gland. With the distribution known, the physician can designate targets within the prostate and then accurately and consistently sample these targets to diagnose clinically important cancers.

Development of such a tumor distribution map (ie, a cancer atlas of the prostate) involves examination of whole-mounted radical prostatectomy specimens and accurate superimposition of 3D image data (Figure 3).[35] Because different prostates have different 3D shapes, a key problem in this superimposition is registration or normalization of the 3D spatial information. The scanned and reconstructed prostate models need to be reshaped such that the lesions are placed in a canonical framework and the corresponding anatomic structures can be compared. Previously, researchers manually registered 2D slices[36] or classified the models into small, medium, and large groups and reshaped all models into one of these groups.[37] Novel computer algorithms have been developed[11,38] to replace the manual processes, which are not only time-consuming and tedious but also subjective. This new development uses a systematic, operator-independent, and single-framework method to accurately map such probabilities to construct an atlas (Figure 4). This atlas has parameters consisting of race, age, and serum PSA level such that a probability map will be generated according to patient-specific prostate parameters.

After the probability map is registered with and overlaid onto a patient's segmented prostate image, the next step is to select regions for biopsy that will best describe the status of the cancer. Using the map, it is easy to choose the first biopsy location by selecting the region with the highest probability in the map. However, selecting the remaining sites is not straightforward because the subsequent high-probability sites most likely lie next to the first site. Zhan et al[11] described an algorithm that enables the physician to sequentially select statistically independent regions to maximize the chance of finding cancer with K number of needles. Based on K and the needle core dimension, a minimization function was established to calculate the orientation and location of the biopsy cores inside the prostate capsule. This optimization scheme picks uncorrelated cancer zones so that a conditional probability is calculated, taking into account the previous needle positions. With this sequential optimization method, globally optimal solutions are found for maximizing the cancer detection rate.

A different type of probability optimization can be planned on the basis of the Gleason grade for finding aggressive cancer, that is, cancer with a Gleason pattern of 4 or 5, instead of merely detecting whether any carcinoma exists. Because finding clinically important cancer leads to more efficient patient treatment, a different yet more difficult goal is to find the extent and expansion rate of cancer. Although still based on this statistical atlas, a different biopsy scheme other than the current standard of care may be needed for this purpose.

Future Applications

Fusion of Molecular Techniques

Because the sensitivity and specificity of the PSA test are low for optimum cancer diagnosis, other molecular diagnostic methods have been sought. For example, in prostate cancer, prostate volume, PSA density, PSA velocity, molecular levels (proteomics),[39] messenger RNA concentrations,[40] and fusion of oncogenes[41] can be integrated into a complex model for improved cancer diagnosis. Potentially, these indicators could prompt improved biopsy schemata for ascertaining the diagnosis. Fusion of aberrant molecular markers with the reconstructed 3D prostate may provide cellular- and molecular-level cancer information. Integration of these indicators of disease into the 3D organ model will likely improve diagnosis and treatment.

Fusion of Image Modalities

Although transrectal sonography is the commonly used imaging technique to identify anatomic landmarks of the prostate gland, it does not provide information regarding tissue morphologic characteristics for localized or advanced disease. Computed tomography (CT),

magnetic resonance imaging (MRI), bone scintigraphy, and positron emission tomography (PET) are frequently used to determine the extent of the cancer.[42] When there is gross extra-capsular extension, lymph node metastasis, and seminal vesicle invasion, cancer extending into adjacent regions can be detected with CT.[43] Magnetic resonance imaging and MR spectroscopic imaging can show the spatial distribution of metabolites (citrate, creatine, choline, and polyamines) that are specific to prostate cancer. Currently, 3D proton MR spectroscopy can map the entire prostate with a resolution of 0.24 mL.[42] With this excellent resolution, it could be a very useful tool for accurately localizing prostate cancer. Another useful imaging technology in cancer detection is elastography. In elastography, elastograms are images that relate to local strains. Because these elasticity parameters are not directly correlated with sonographic parameters, elastography provides new structural information.[13,14] In nuclear medicine, Moses et al[44] (Lawrence Berkeley National Laboratory, Berkeley, CA) built a prototype PET scanner exclusively for prostate cancer imaging. Each of the above imaging modalities has different advantages and may be able to depict cancers more effectively than sonography. Fusion of them with 3D sonography may increase the yield over probability mapping alone. Therefore, physicians can use this synergistic fusion method to help determine appropriate treatment strategies and management plans.

Tracking of Disease Progression

With the full 3D spatial information mapped, a fourth dimension can be added to track the advances or retractions of prostate cancer over time. Active surveillance, watchful waiting, additional biopsies, and monitoring of treatment results can all be easily and systematically implemented because the spatiotemporal dynamics of the prostate can be tracked.

With 3D image acquisition, tracking of the ultrasound probe and processing techniques comparing the progression of the disease can be relatively easy. Therapies can be offered once the monitored tumor needs to be treated. Similarly, the locations of the cores from previous biopsies can be recorded and saved. For subsequent biopsy procedures, the current status of the prostate can be obtained by imaging, segmentation, and registration to the older images, and new biopsy targets can be planned accordingly (Figure 5). The effectiveness of chemical, radiation, and other treatments can also be studied by knowing the precise location of the tumor, facilitating the ability to return to the initial sites for sampling and allowing one to follow the Gleason score, core percentage, and number over time. Therefore, the aggressiveness of the cancer can be ascertained, and different treatments can be prescribed according to different individual cases.

Three-Dimensional Cancer Therapy

Therapies for localized prostate cancer include surgery, external beam radiotherapy, brachytherapy, high-intensity focused ultrasound, and cryotherapy. The efficacy of all of these treatments, except for surgery, can be improved considerably on 3D rather than 2D imaging. Analogous to the planning of biopsy sites, the locations of the radiation foci, cryotherapy, and implanted seeds must be optimized to ablate the prostate gland while sparing adjacent healthy tissue and the neurovascular bundle. Fusion of MRI, CT, and transrectal sonography will provide better knowledge of the disease, and the treatment burden will be better defined.

Several companies in the United States and Europe have commercialized devices for 3D guidance. SPOT PRO by Nucletron (Veenendaal, the Netherlands) is a mobile cart that offers live planning with 3D needle guidance and real-time dosimetry updates.[45] It has automated features for contouring, planning, and seed detection. It also has a needle navigator that dynamically illuminates needle pathways. It shows live sagittal and transverse

images and provides visual feedback of the needle's depth and direction. VariSeed by Varian Medical Systems (Palo Alto, CA) is a software application for planning seed treatment.[46] It can be used in conjunction with hardware for TRUS-guided transperineal seed implant brachytherapy. It contains modules for image acquisition, patient data management, preplanning and postplanning, 3D image registration, fusion with CT data, dose optimization, and nomogram planning for needle positioning. VariSeed also has different modules for permanent and temporary seeding plans. Sononav by Medtronic (Louisville, CO) is an imaging system that correlates preoperative MRI or CT scans to intraoperative sonographic videos to provide real-time image updates.[47] The main applications are determination of the completeness of tumor resections and brain shift phenomenon during neurologic operations. Sononav can automatically reformat preoperative images on the basis of the current sonograms. It is compatible with multiple vendors of ultrasound probes. The companies mentioned above support the conclusion that prostate cancer represents an expanding market, and sonography is a renewed imaging modality because of its low cost and noninvasiveness.

Conclusions

Accurate 3D cancer identification and needle navigation are paramount in image-guided procedures for the prostate. This 3D approach has potential for better disease diagnosis and therapy. Additionally, when fusing together different imaging modalities such as CT, MRI, MR spectroscopy, elastography, and PET, physicians can better identify targets that are likely to host cancerous tissue.

As computers continue to advance in power, full 3D spatial information of the prostate gland can be obtained within seconds when tracking of the image acquisition is accomplished. However, it still may not be enough speed for real-time intraoperative procedures such as on-the-fly patient motion correction. Advances in programming with general-purpose graphics processing units promises more than an order of magnitude increase in image processing speed. When successful, a time dimension can be added to interventional procedures, rendering them in 4 dimensions (3D space plus time). As the time dimension is extended and image segmentation and registration techniques mature, physicians can accurately track the progress of the disease and the efficacy of treatments. With information on the anatomic, metabolic, functional, biochemical, and biomechanical statuses of different regions of the entire gland, prostate cancers will be better diagnosed and treated. The work flow of diagnosis and treatment procedures will continue to improve, and cost will continue to decrease, along with an improved understanding of the spatiotemporal dynamics of this prevalent disease.

Abbreviations

CT	computed tomography
MR	magnetic resonance
MRI	magnetic resonance imaging
PET	positron emission tomography
PSA	prostate-specific antigen
3D	3-dimensional
TRUS	transrectal ultrasound
2D	2-dimensional

References

1. Jemal A, Siegel R, Ward E, Murray T, Xu J, Thun MJ. Cancer statistics, 2007. CA Cancer J Clin. 2007; 57:43–66. [PubMed: 17237035]
2. Lee F, Torp-Pedersen ST, McLeary RD. Diagnosis of prostate cancer by transrectal ultrasound. Urol Clin North Am. 1989; 16:663–673. [PubMed: 2479161]
3. American Cancer Society. Detailed guide: prostate cancer. http://www.cancer.org/docroot/CRI/CRI_2_3x.asp?dt=36.
4. US Cancer Statistics Working Group. United States Cancer Statistics 2003 Incidence and Mortality. Department of Health and Human Services, Centers for Disease Control and Prevention, National Cancer Institute; Atlanta, GA. 2007.
5. Gleason DF, Mellinger GT. Prediction of prognosis for prostatic adenocarcinoma by combined histological grading and clinical staging. J Urol. 1974; 111:58–64. [PubMed: 4813554]
6. Greene, FL.; Page, DL.; Fleming, ID.; Fritz, A.; Balch, CM.; Haller, DG. AJCC Cancer Staging Manual. 6th ed.. London, England: Springer; 2002.
7. Hodge KK, McNeal JE, Terris MK, Stamey TA. Random systematic versus directed ultrasound guided transrectal core biopsies of the prostate. J Urol. 1989; 142:71–75. [PubMed: 2659827]
8. Djavan B, Ravery V, Zlotta A, et al. Prospective evaluation of prostate cancer detected on biopsies 1, 2, 3, and 4: when should we stop? J Urol. 2001; 166:1679–1683. [PubMed: 11586201]
9. Roehl KA, Antenor JA, Catalona WJ. Serial biopsy results in prostate cancer screening study. J Urol. 2002; 167:2435–2439. [PubMed: 11992052]
10. Stewart CS, Leibovich BC, Weaver AL, Lieber MM. Prostate cancer diagnosis using a saturation needle biopsy technique after previous negative sextant biopsies. J Urol. 2001; 166:86–92. [PubMed: 11435830]
11. Zhan Y, Shen D, Zeng J, et al. Targeted prostate biopsy using statistical image analysis. IEEE Trans Med Imaging. 2007; 26:779–788. [PubMed: 17679329]
12. Swanson MG, Zektzer AS, Tabatabai ZL, et al. Quantitative analysis of prostate metabolites using 1H HR-MAS spectroscopy. Magn Reson Med. 2006; 55:1257–1264. [PubMed: 16685733]
13. Ophir J, Alam SK, Garra BS, et al. Elastography: imaging the elastic properties of soft tissues with ultrasound. J Med Ultrasonics. 2002; 29:155–171.
14. Souchon R, Rouvière O, Gelet A, et al. Visualisation of HIFU lesions using elastography of the human prostate in vivo: preliminary results. Ultrasound Med Biol. 2003; 29:1007–1015. [PubMed: 12878247]
15. Elliot TL, Downey DB, Tong S, McLean CA, Fenster A. Accuracy of prostate volume measurements in vitro using three-dimensional ultrasound. Acad Radiol. 1996; 3:401–406. [PubMed: 8796692]
16. Tong S, Downey DB, Cardinal HN, Fenster A. A three-dimensional ultrasound prostate imaging system. Ultrasound Med Biol. 1996; 22:735–746. [PubMed: 8865568]
17. Barqawi, AB.; Li, L.; Crawford, ED.; Suri, J. Semi-automated vs automated prostate boundary estimation from 3-D transrectal ultrasound images. Paper presented at 2007 Computer-Assisted Radiology and Surgery Conference; Berlin, Germany. 2007.
18. Cool D, Downey D, Izawa J, Chin J, Fenster A. 3D prostate model formation from non-parallel 2D ultrasound biopsy images. Med Image Anal. 2006; 10:875–887. [PubMed: 17097333]
19. Kumar, D.; Shen, D.; Wei, L.; Turlapati, R.; Suri, J. Motion correction strategies for interventional angiography images: a comparative approach. Paper presented at: IEEE International Conference on Imaging Processing; San Antonio TX. 2007.
20. Wang Y, Cardinal HN, Downey DB, Fenster A. Semiautomatic three-dimensional segmentation of the prostate using two-dimensional ultrasound images. Med Phys. 2003; 30:887–897. [PubMed: 12772997]
21. Wei Z, Wan G, Gardi L, Mills G, Downey D, Fenster A. Robot-assisted 3D-TRUS guided prostate brachytherapy: system integration and validation. Med Phys. 2004; 31:539–548. [PubMed: 15070252]
22. Andriole, GL.; Williams, ER. US Genitourinary Disease. London, England: Touch Briefings; 2006 Jun. The utilization of ultrasound in the diagnosis of carcinoma of the prostate; p. 28

23. Taneja SS. Prostate biopsy: targeting cancer for detection and therapy. Rev Urol. 2006; 8:173–182. [PubMed: 17192796]
24. Park SB, Kim JK, Choi SH, Noh HN, Ji EK, Cho KS. Prostate volume measurement by TRUS using heights obtained by transaxial and midsagittal scanning: comparison with specimen volume following radical prostatectomy. Korean J Radiol. 2000; 1:110–113. [PubMed: 11752939]
25. Tong S, Cardinal HN, McLoughlin RF, Downey DB, Fenster A. Intra- and inter-observer variability and reliability of prostate volume measurement via two-dimensional and three-dimensional ultrasound imaging. Ultrasound Med Biol. 1998; 24:673–681. [PubMed: 9695270]
26. Chan T, Vese L. Active contours without edges. IEEE Trans Image Process. 2001; 10:266–277. [PubMed: 18249617]
27. Li, C.; Xu, C.; Gui, C.; Fox, MD. Level set evolution without reinitialization: a new variational formulation. Proceedings of the IEEE International Conference on Computer Vision and Pattern Recognition; Institute of Electrical and Electronics Engineers; Piscataway, NJ. 2005. p. 430-436.
28. Barqawi AB, Li L, Crawford ED, et al. Three Different Strategies for Real-Time Prostate Capsule Volume Computation from 3-D End-Fire Transrectal Ultrasound. Conf Proc IEEE Eng Med Biol Soc. 2007; 2007:816–818. [PubMed: 18002081]
29. Paul R, Schöler S, van Randenborgh H, et al. Optimization of prostatic biopsy: a prospective randomized trial comparing the sextant biopsy with a 10-core biopsy. Impact of prostatic region of sampling. Urol Int. 2005; 74:203–208. [PubMed: 15812204]
30. Naughton CK, Miller DC, Mager DE, Ornstein DK, Catalona WJ. A prospective randomized trial comparing 6 versus 12 prostate biopsy cores: impact on cancer detection. J Urol. 2000; 164:388–392. [PubMed: 10893592]
31. Chen ME, Troncoso P, Tang K, Babaian RJ, Johnston D. Comparison of prostate biopsy schemes by computer simulation. Urology. 1999; 53:951–960. [PubMed: 10223489]
32. Chen ME, Troncoso P, Johnston DA, Tang K, Babaian RJ. Optimization of prostate biopsy strategy using computer based analysis. J Urol. 1997; 158:2168–2175. [PubMed: 9366337]
33. Eskew LA, Bare RL, McCullough DL. Systematic 5 region prostate biopsy is superior to sextant method for diagnosing carcinoma of the prostate. J Urol. 1997; 157:199–203. [PubMed: 8976250]
34. Opell MB, Zeng J, Bauer JJ, et al. Investigating the distribution of prostate cancer using three-dimensional computer simulation. Prostate Cancer Prostatic Dis. 2002; 5:204–208. [PubMed: 12496982]
35. Zeng J, Bauer JJ, Mun SK. Modeling and mapping of prostate cancer. Comput Graph. 2000; 24:683–694.
36. Xuan J, Wang Y, Sesterhenn IA, Moul JW, Mun SK. 3D model supported prostate biopsy simulation and evaluation. Notes Comput Sci. 1998; 1496:358–367.
37. Frimmel H, Egevad L, Bengtsson E, Busch C. Modeling prostate cancer distributions. Urology. 1999; 54:1028–1034. [PubMed: 10604703]
38. Shen D, Lao Z, Zeng J, et al. Optimized prostate biopsy via a statistical atlas of cancer spatial distribution. Med Image Anal. 2004; 8:139–150. [PubMed: 15063863]
39. Schostak M, Schwall G, Poznanovic S, et al. Annexin A3 quantification from supernatants of urine after DRE provides a novel and clinically easy available biomarker for the non-invasive diagnosis of prostate cancer [abstract]. J Urol. 2007; 177(suppl):470.
40. DiagnoCure. Prostate cancer diagnosis. http://www.diagnocure.com/en/products-projects/prostate-cancer/prostate-cancer.php.
41. Meyerson M. Cancer: broken genes in solid tumours. Nature. 2007; 448:545–546. [PubMed: 17671492]
42. Akin O, Hricak H. Imaging of prostate cancer. Radiol Clin North Am. 2007; 45:207–222. [PubMed: 17157630]
43. Yu KK, Hricak H. Imaging prostate cancer. Radiol Clin North Am. 2000; 38:59–85. viii. [PubMed: 10664667]
44. Moses, WW.; Huber, J. Dedicated PET instrumentation for prostate imaging. Paper presented at: Advanced Molecular Imaging Techniques in the Detection, Diagnosis, Therapy, and Follow-up of Prostate Cancer; December 6–7, 2005; Rome, Italy.

45. Nucletron BV. Products & solutions. https://www.nucletron.com.
46. Varian Medical Systems. VariSeed. http://www.varian.com/us/oncology/brachytherapy/variseed.html.
47. Medtronic Inc. About Medtronic Navigation: intra-operative imaging and navigation. http://www.medtronicnavigation.com/about.

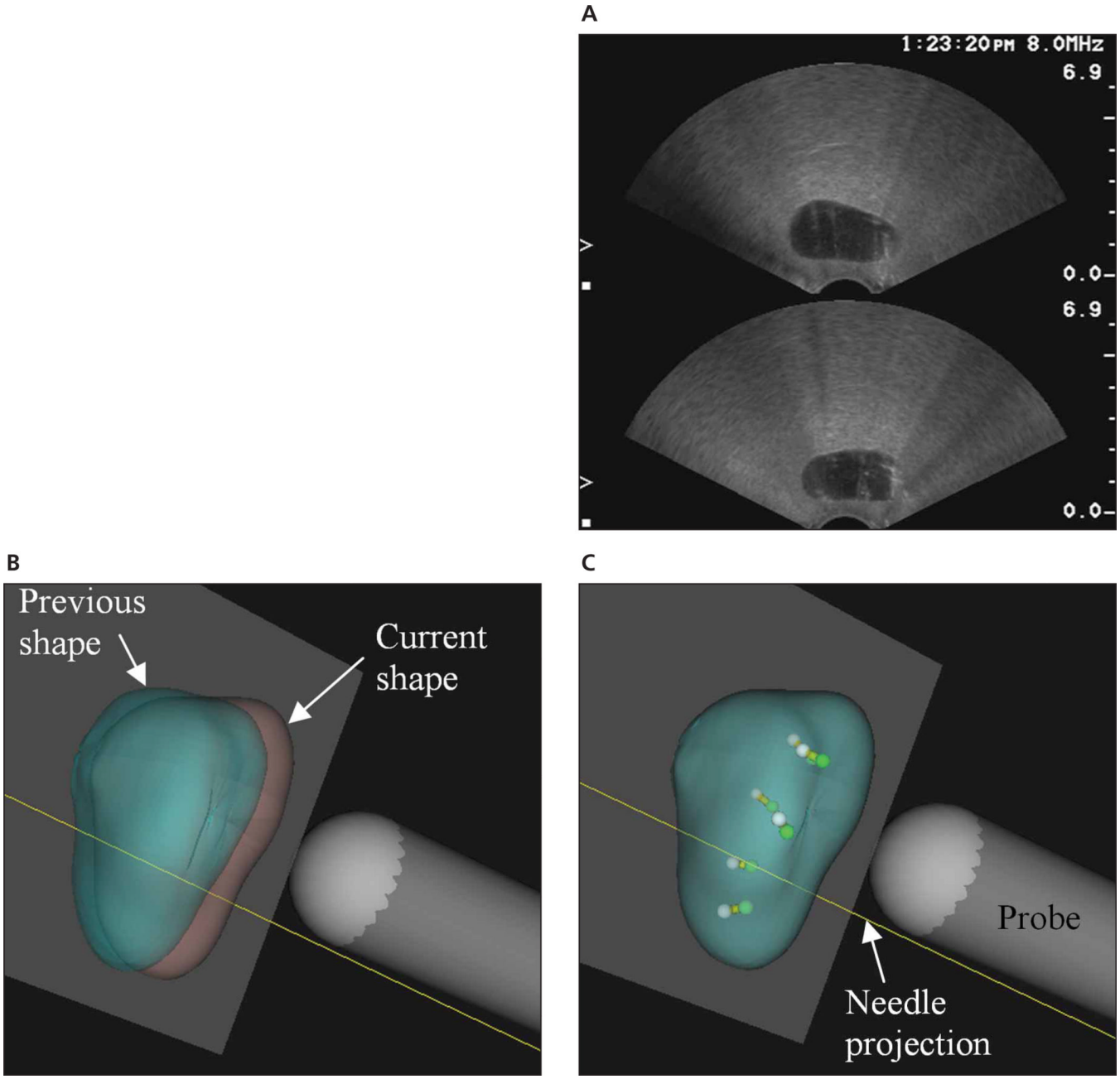

Figure 1.
Comparison between 2D and 3D displays of biopsy procedures. **A**, Screen capture of sonograms of a prostate phantom. Only 2 views, transverse (top) and sagittal (bottom), are visible. **B** and **C**, Screen captures from the Eigen Artemis system showing a subsequent biopsy procedure. **B**, Unregistered previous (green) and current (pink) volumes. **C**, Registered volumes with previous (white) and current (green) core locations inside.

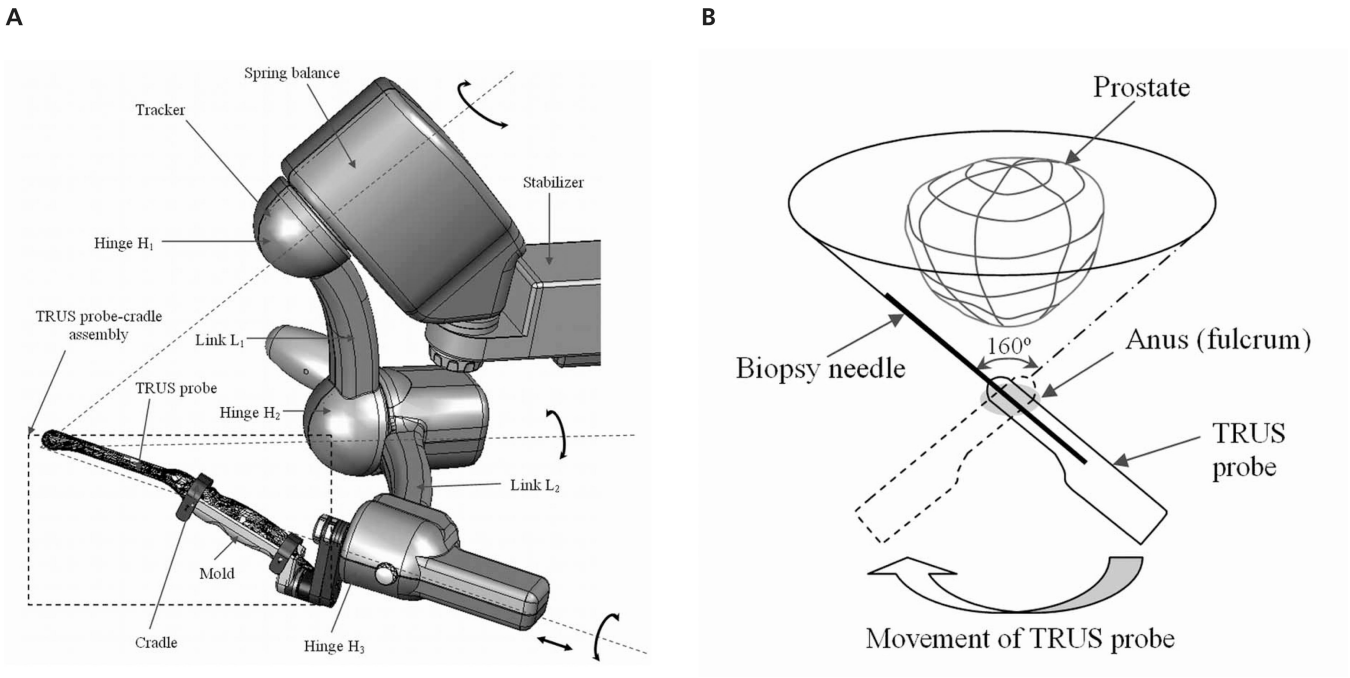

Figure 2.

A, Eigen electromechanical tracker. It has 4° of freedom with a fulcrum for TRUS-guided biopsy. **B**, With the end-firing ultrasound probe, there is wide needle coverage of the prostate by rotation of the transducer probe (as indicated by the broad curved arrow at the bottom) with the anus as a fulcrum. The dashed probe outline shows the TRUS probe at the left extreme position. The biopsy needle is straight so that the range of motion that it spans makes a cone shape with an angle of 160°.

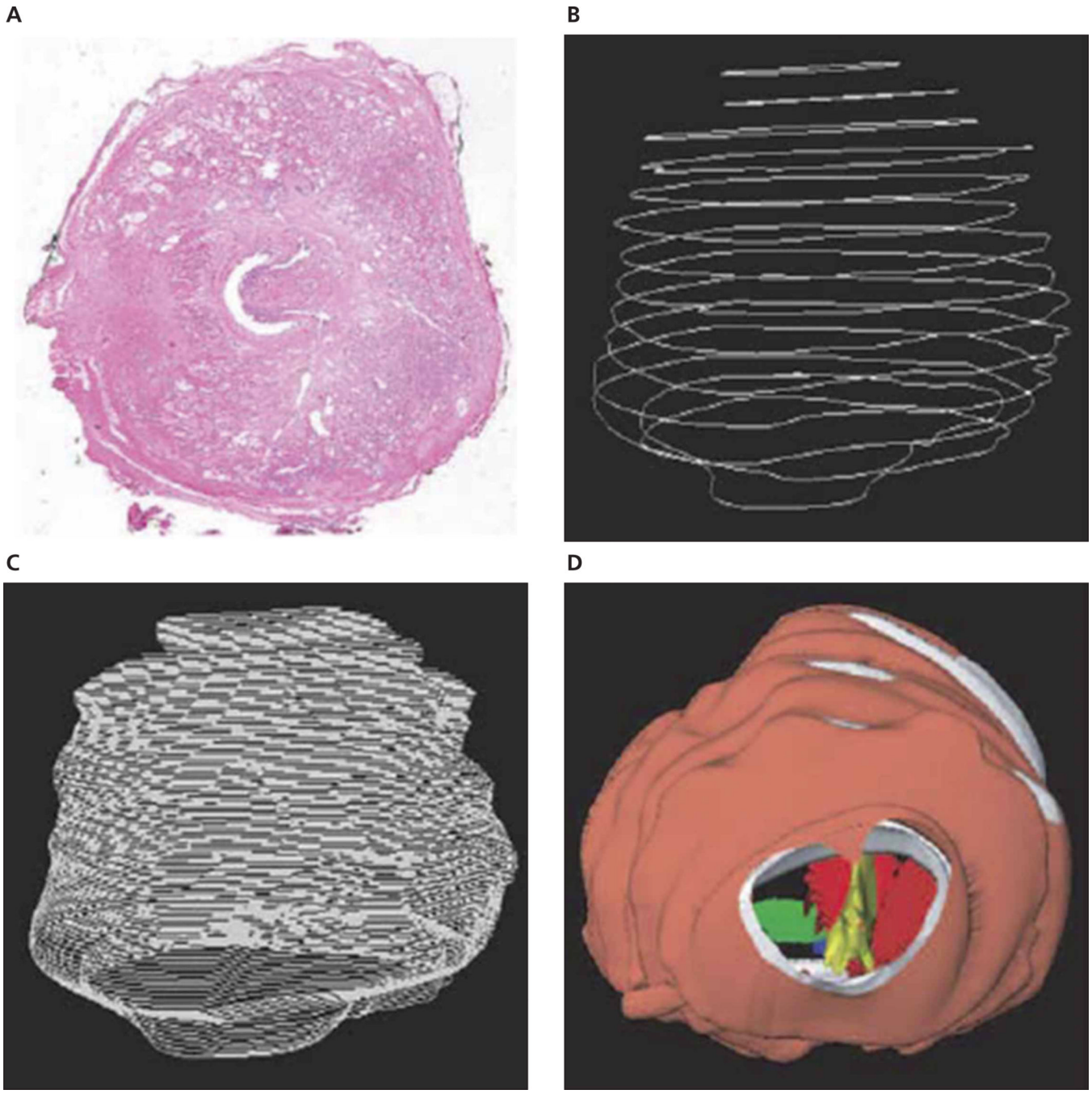

Figure 3.
Three-dimensional reconstruction of prostate models. **A**, Digitized image of a single slice of a step-sectioned radical prostatectomy specimen. **B**, Stacked surgical margin contour controls of original slices. **C**, Surgical margin contour interpolation. **D**, Three-dimensional reconstructed prostate model.35

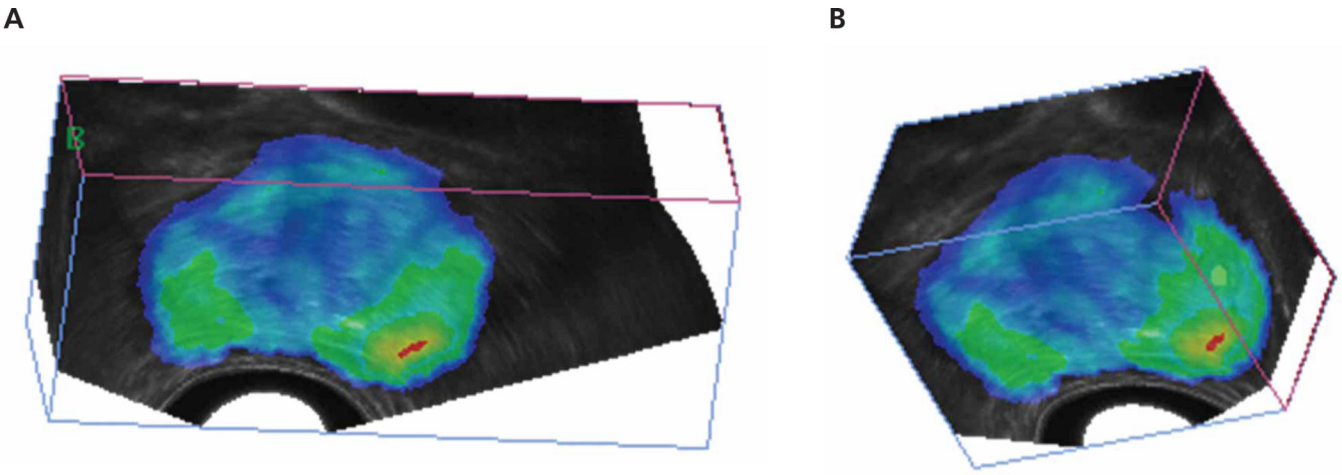

Figure 4.
Cancer probability map overlaid onto 3D sonograms. **A** and **B**, Two different views of the same prostate atlas. Colors represent the probability of cancer.

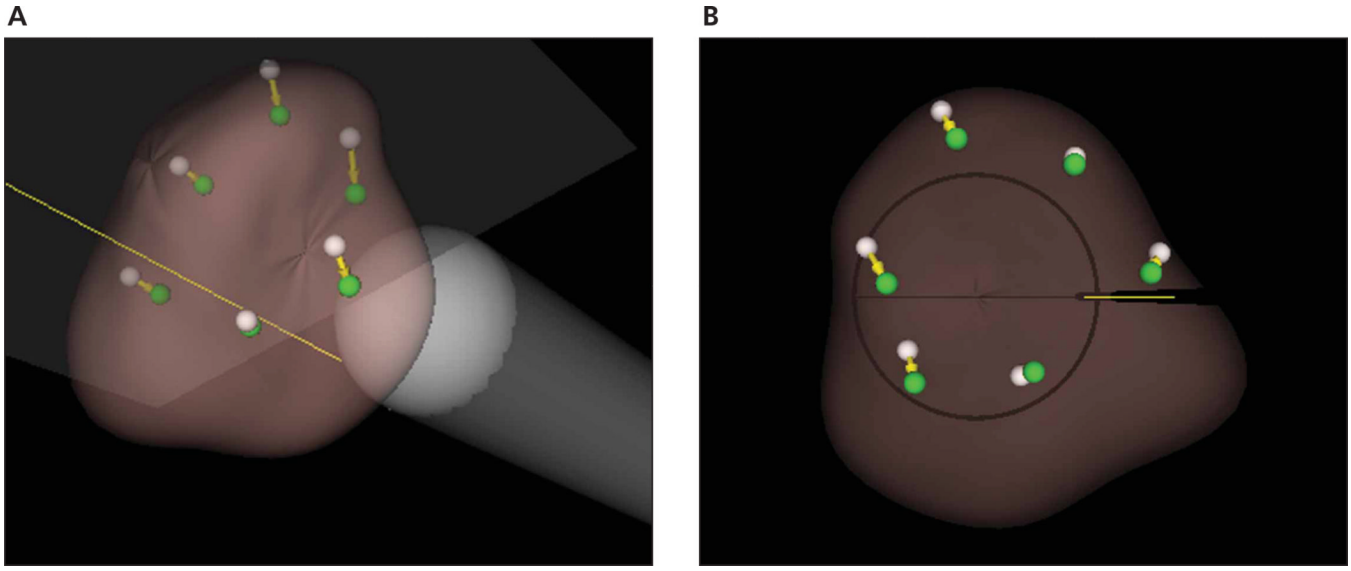

Figure 5.
Simulated tracking targets in repeated biopsy. **A**, Screen capture from the Eigen software showing sextant biopsies (white, old; and green, new) in an oblique view. **B**, Bottom view.